

# Numerical Simulation of Natural Ventilation Performance of Solar Chimney with Built-in Phase Change Material

N. Ochiai, K. Sagara, T. Yamanaka, H. Kotani, and Y. Momoi

*Osaka University*

Y. Kaneko

*Kajima Corporation*

## ABSTRACT

This paper presents a study of solar chimneys using a Phase Change Material (PCM) integrated into the heat absorber of the solar chimney. Solar chimneys have recently been used as natural ventilation devices in buildings in order to improve the quality of indoor air and provide a comfortable environment for the inhabitants. The advantage of a solar chimney is that it depends on solar energy rather than electricity for generating ventilation. However, it is unstable as a ventilation system since its ventilation rate is directly affected by the solar radiation. In order to solve this problem, the method of incorporating PCM into the solar chimney was developed and its usability has been investigated in previous studies. This paper focuses on the characteristics of PCM, especially on the super-cooling during the solidifying process. Experiments were conducted to understand the thermophysical properties of PCM and numerical simulations which take the effect of super-cooling of PCM in consideration were developed. Further, a model for predicting the ventilation rate of the solar chimney with built-in PCM was developed and the simulation results were compared with the experimental results in order to evaluate the accuracy of the model.

## 1. INTRODUCTION

The integration of PCM into building elements such as walls, floors and air distribution systems is a well established subject and has been investigated for passive thermal storage.

The review by Tyagi et al (2007) on various possible methods for heating and cooling in buildings is one example. PCM is a substance with a high heat of fusion which is capable of storing and releasing large amounts of energy during melting and solidifying processes at certain temperatures and it exhibits a rather slow thermal response. The authors focused on these features of PCM and a prototype of a solar chimney with built-in PCM (Fig.1) was developed, aiming to realize a 24-hour ventilation system (Kaneko et al, 2005). Sodium sulfate decahydrate ( $\text{Na}_2\text{SO}_4 \cdot 10\text{H}_2\text{O}$ ; melting point 32 degrees C, freezing point 30 degrees C, latent heat of fusion 126 kJ/kg) was used for latent heat storage and was incorporated behind a black coated aluminum (Al) panel in the wall of the solar chimney. It is expected that heat storage in PCM and ventilation occur in daytime and that evening/night ventilation is induced mainly by discharge of the latent heat stored in PCM. This stored heat is transferred to the air flowing over the Al panel and is used to contribute to the temperature difference between the air flowing through the chimney and the ambient air in the evening or at the other times when there is no solar radiation.



Fig.1. The prototype of the solar chimney with built-in PCM.

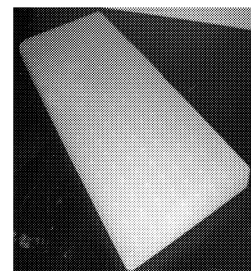


Fig.2. PCM panel.

## 2. THERMAL PROPERTIES OF PCM

An experiment was conducted in order to investigate the thermal characteristics of PCM in detail. The PCM used in this study was sodium sulfate decahydrate which was encapsulated in a flat rectangular polypropylene container (size:  $250 \times 600 \times 25$  mm) as shown in Fig.2.

### Experimental Setup

Schematic diagram of the experimental setup is shown in Fig.3, and properties of the materials are listed in Table1. PCM was insulated by a polystyrene board and the apparatus was set up in an artificial climate chamber in which the room air temperature was controlled to be 10 degrees C. The surface of the PCM panel was heated up by an electronic heating sheet until

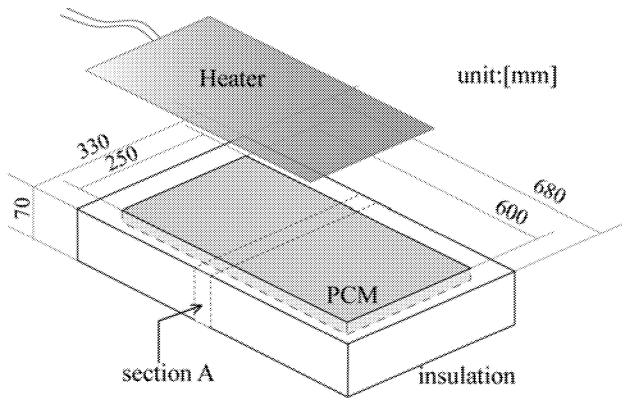


Fig.3. A schematic diagram of the apparatus.

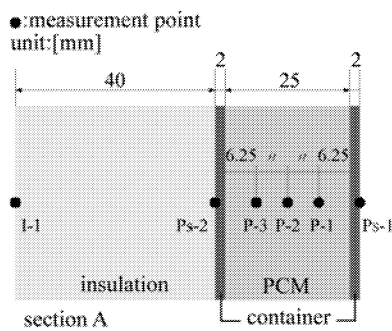


Fig.4. The temperature measurement points.

Table1. The properties of the materials.

Materials	$x$ (mm)	$\rho$ (kg/m <sup>3</sup> )	$C_p$ (kJ/kgK)	$k$ (W/mK)
Insulation	40	30	0.0014	0.03
Container	2	910	0.0017	0.13
PCM(Solid)	25	1390	3.6	0.19
PCM(Liquid)	25	1410	3.5	0.22

Melting point : 32 degrees C, Freezing point: 30 degrees C, Heat of Fusion : 126kJ/kg  
 Note:  $x$ ,  $\rho$ ,  $C_p$ , and  $k$  are thickness, density, specific heat and thermal conductivity of the materials, respectively.

the PCM was completely melted. Then the electronic heating sheet was removed and the PCM panel was naturally cooled down inside the chamber. Seventy-seven T-type calibrated thermocouples with the accuracy of  $\pm 0.2$  degrees C were used to measure the temperatures of the various elements of the apparatus. The measurement points are shown in Fig.4.

### Results of the experiment

PCM was heated during 3.5 hours and thereafter cooled down during 15.5 hours in the artificial climate chamber. As can be seen in Fig.5, the temperature change of PCM is small around 30 degrees C because of the phase transition of PCM. The slow temperature change continued for about 5 hours.

A close look at the super-cooling period is shown in Fig.6 and the temperature distributions of PCM at various times are shown in Fig.7. Super-cooling could be observed when the temperature of P-1 reached

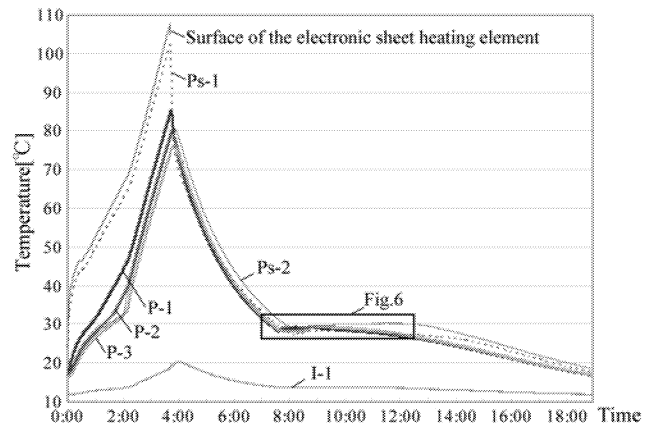


Fig.5. Temperature history of the apparatus.

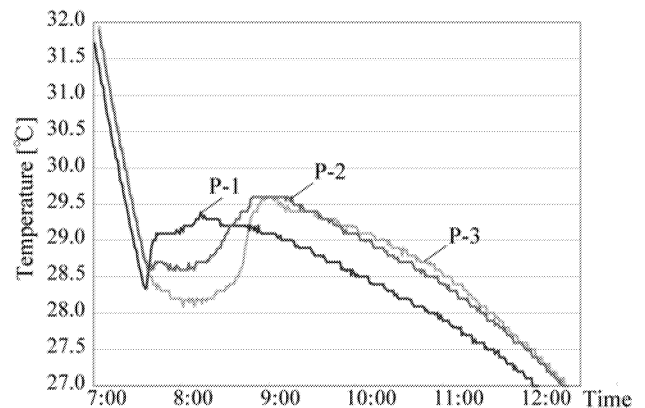


Fig.6. A closer look at the super-cooling in the PCM.

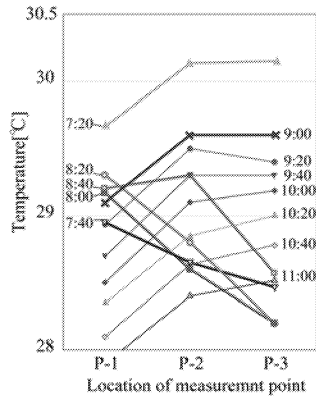


Fig.7. The temperature distribution of PCM.

to 28.3 degrees C, after which its temperature rose to 29.1 degrees C. The temperatures of P-2 and P-3, on the other hand, were descending continuously until they reached 28.6 and 28.2 degrees C respectively. It was therefore found that super-cooling of PCM occurs heterogeneously in the apparatus.

### 3. METHOD OF SIMULATION

#### *Numerical model*

An enthalpy method (Saito, 1992) was applied in the numerical simulation. The governing equation is;

$$\rho_x \frac{\partial H}{\partial t} = k \frac{\partial^2 \theta}{\partial x^2} \quad (1)$$

$$H = \int C_{p,pcm} d\theta \quad (2)$$

where  $\rho$  is the density  $\text{kg/m}^3$ ,  $H$  the enthalpy  $\text{kJ/kg}$ ,  $k$  the thermal conductivity  $\text{kW/mK}$  and  $\theta$  the temperature  $\text{K}$ ,  $C_{p,pcm}$  the specific heat of PCM  $\text{kJ/kgK}$ .

The equations were solved by explicit finite difference method. The time step was set to 1 second and PCM was divided into 50 layers, the insulation material into 5 layers and the container into 1 layer.

The following conditions were assumed; (1) heat transfer through PCM and polypropylene container is one dimensional; (2) when PCM is in melting or freezing process, specific heat of PCM changes to follow a sine curve of the temperature corresponding to the latent heat (Fig.8); (3) convection and radiation on the outside surface of the PCM container are ignored.

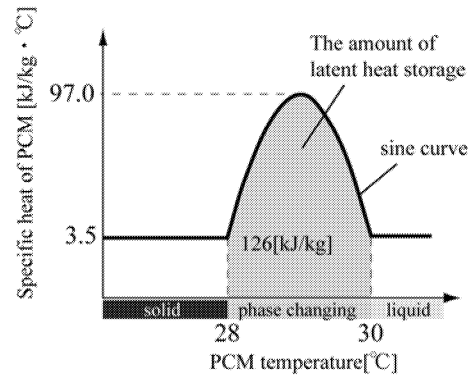


Fig.8. Property of specific heat of PCM.

The measured initial temperatures in the experiment were used as initial condition of the calculation. The calculation was conducted only for the cooling process.

#### *Thermal conductivity of PCM*

At previous studies, the numerical model disagrees with the measured data when the PCM is in liquid phase. It can be assumed that natural convection occurs partly in the PCM, which results in rapid heat transfer.

Therefore, we investigated the effect of natural convection by adjusting the thermal conductivity, which is called equivalent thermal conductivity here. In order to identify a suitable equivalent thermal conductivity of PCM in liquid phase, the simulation results under different equivalent thermal conductivity of liquid phase were compared with the experimental results. The thermal conductivity of liquid phase was set to 0.22 (default), 0.30, 0.50 and 0.60  $\text{W/mK}$ .

The comparisons of the simulation results with the measured data are shown in Fig.9. The simulation results agree with the experimental results for higher thermal conductivity. Therefore, the equivalent thermal conductivity of liquid phase is identified as 0.60  $\text{W/mK}$  in the numerical model.

#### *Super-cooling of PCM*

When super-cooling occurs in PCM, it can be assumed that the temperature of PCM is descending continuously even under freezing point until it reaches to super-cooling-break temperature  $\theta_s$  without changing phase. The supercooled heat  $Q_I$  as shown in Fig.10

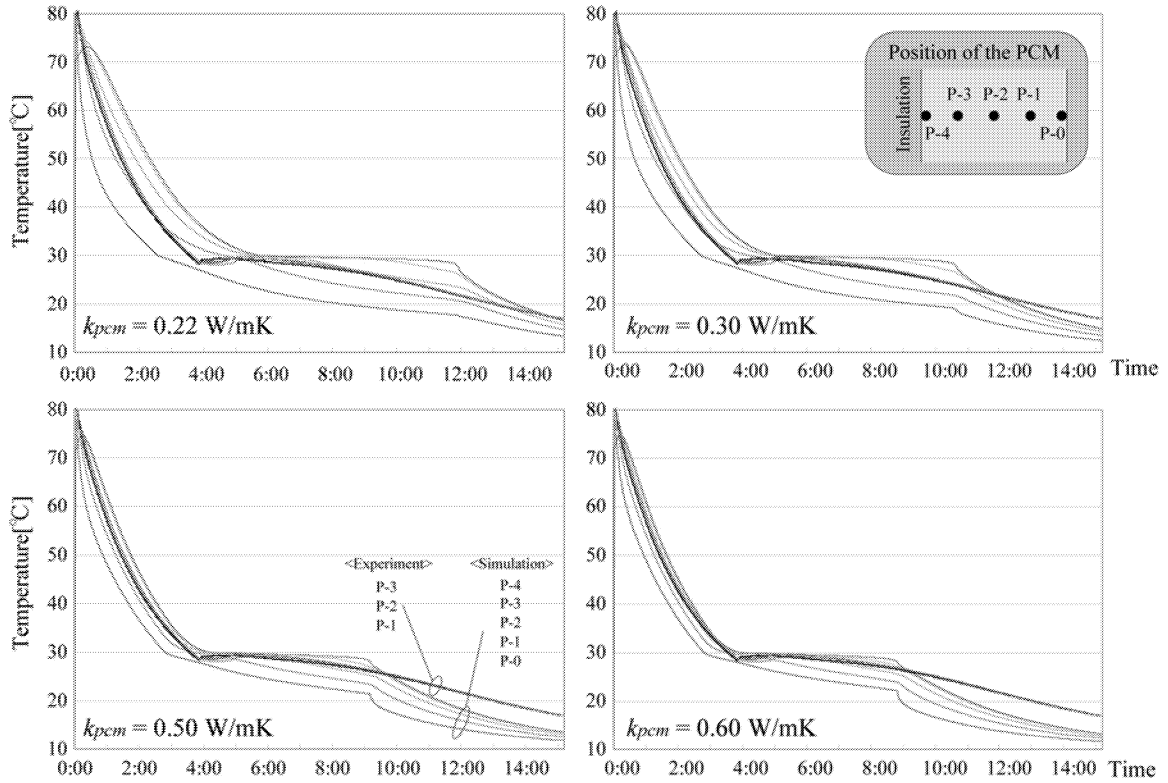


Fig.9. The effect of thermal conductivity of PCM in the simulation.

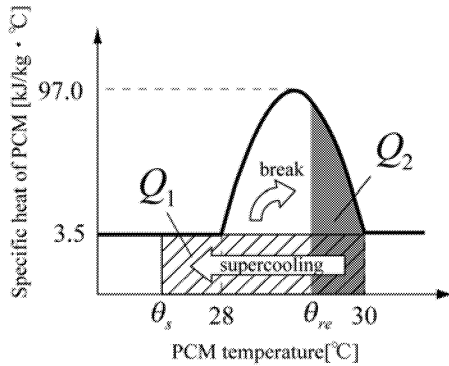


Fig.10. Property of the specific heat in phase change.

corresponds to the sensible heat during super-cooling. After reaching  $\theta_s$ , the temperature of PCM is assumed to jump immediately from  $\theta_s$  to the recover temperature  $\theta_{re}$ . At the same time, the supercooled heat is used for phase transition from liquid to solid, and  $\theta_{re}$  is calculated from the following equations.

$$Q_1 = Q_2 \quad (3)$$

$$Q_1 = \rho_1 C_{p,pcm} (30 - \theta_s) \quad (4)$$

$$Q_2 = \rho_2 \int_{\theta_{re}}^{30} C_{p,pcm}(\theta) d\theta \quad (5)$$

where  $\rho$  is the density of PCM  $\text{kg/m}^3$  and  $C_{p,pcm}$  the specific heat of PCM  $\text{kJ/kgK}$ .

The conditions of PCM shift from the sensible heat discharge to the latent heat discharge after the break of super-cooling, and the specific heat of PCM changes to follow the sine curve of temperature. To simplify the calculations, it is assumed in this study that the break of super-cooling occurs everywhere at the same time when the lowest temperature of PCM reaches to  $\theta_s$ .

### Results and discussions

The simulation results of the temperatures of PCM, where super-cooling-break temperature was set to 26 degrees C is shown in Fig.11. The shaded part of the upper graph is enlarged and shown in the below. It was found that the super-cooling occurs around 3.5h after the start of cooling in the simulation, but the simulation result does not agree well with the measured data after the break of super-cooling. It is likely due to the assumption that the break of super-cooling occurs everywhere at the same time.

Fig.12 shows a comparison of simulation results under different super-cooling-break

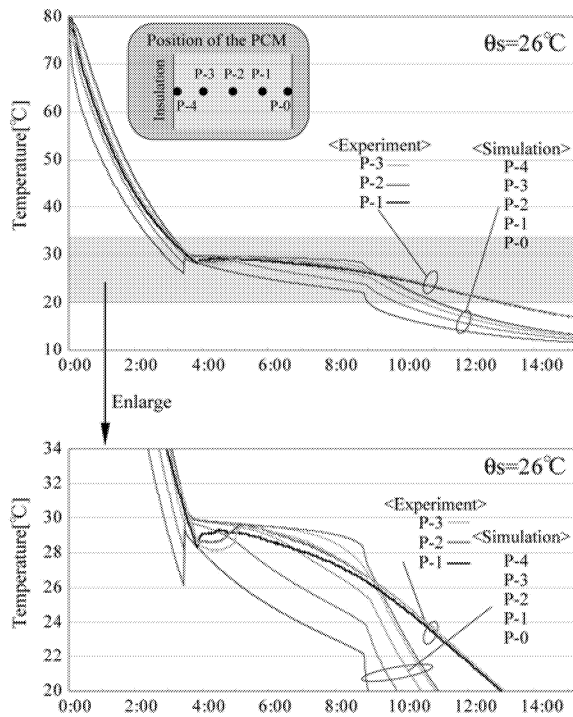


Fig.11. The simulation results of PCM temperature.

temperatures. It was found in the simulation results that the super-cooling does not appear at the insulated side of PCM in case of higher super-cooling-break temperature. This point remains to be solved in the future, and further studies should be carried out to improve the accuracy of the model.

#### 4. STUDY OF THE SOLAR CHIMNEY

##### *Experimental setup*

The prototype of a solar chimney with built-in PCM (Fig.1) was fabricated and installed on the roof of an eight-story building. Six encapsulated PCM panels were incorporated and the dimensions of the prototype was  $1.2 \times 0.75 \times 0.4$  m. It was oriented to face south and tilted 45 degrees with respect to the horizon. Fig.13 shows the measured temperature of the inside PCM and the surface of the Al panel. The experiment was conducted on 25-29 May 2005 and the outdoor conditions are shown in Fig.14.

From Fig.13, it can be found that the temperature change of PCM is small around 30 degrees C because of phase transition and that the temperature of the Al panel is affected by

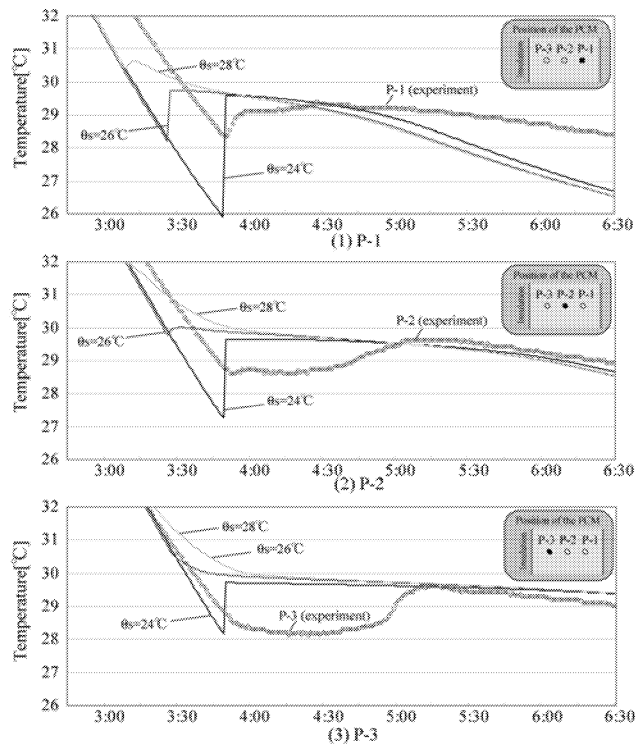


Fig.12. The comparison of the simulation results under the different super-cooling break temperature.

the temperature change of PCM.

##### *Simulation of Solar Chimney*

A numerical simulation model (Adam, 2002) to predict the ventilation rate of the solar chimney was applied. The method of simulating the phase transition was the same as mentioned above in Chapter 3. In these calculations, PCM was divided into 10 layers, the Al panel into 1 layer, the polypropylene container into 1 layer and the insulation material into 5 layers. The air volume inside the chimney was divided into 24 blocks along the direction of air flow. Super-cooling-break temperature was set to 26 degrees C and the inputs for the calculation were the incident solar radiation and ambient air temperature.

Fig.15 shows the simulation results of the solar chimney. The simulation results agree well with the measured data in general. It can be found that the ventilation rate through the solar chimney maintains more than  $110 \text{ m}^3/\text{h}$  in the evening/night except for the time period of super-cooling, and the difference of ventilation rate between the two cases with/without super-cooling was  $10\text{-}20 \text{ m}^3/\text{h}$ .

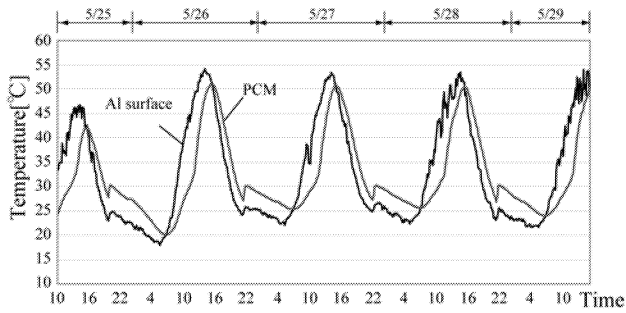


Fig.13. The measured data of PCM temperature (at the middle of the PCM panel set in the solar chimney).

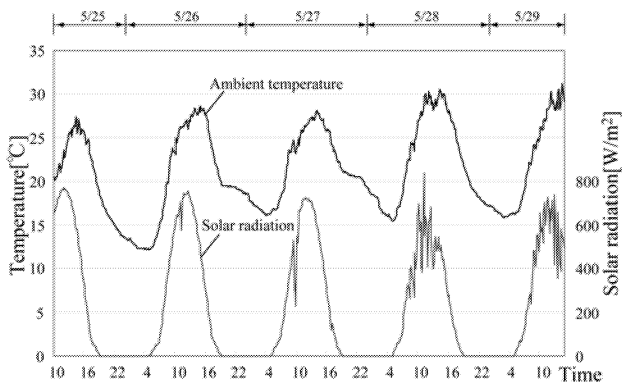


Fig.14. Outdoor conditions on 25-29 May 2005.

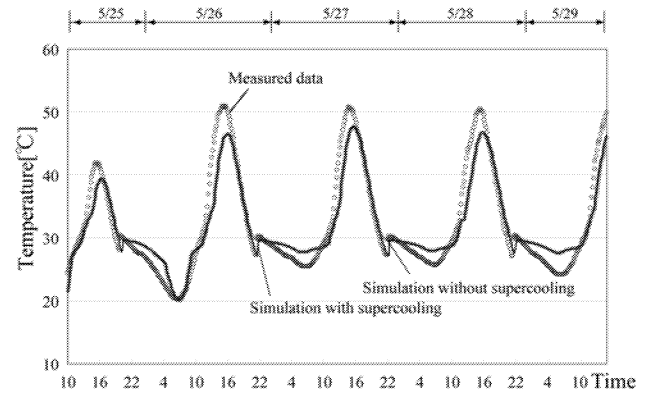
## 5. CONCLUSIONS

The thermal performance of PCM during phase transition has been studied experimentally and numerically. The experimental results show that super-cooling was observed in the freezing process of PCM, and a super-cooling model was introduced into the phase change simulation of PCM in this study. The simulation results agree qualitatively with the experimental data, but there are some challenges in order to improve the model accuracy.

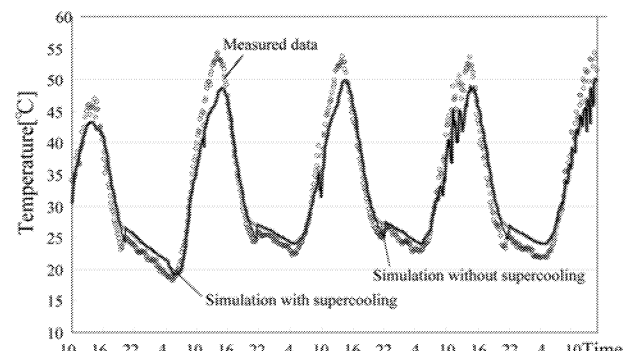
The prototype of a solar chimney with built-in PCM was fabricated and experimental and numerical studies were conducted. It can be concluded that the PCM integrated into solar chimney showed a positive influence on the ventilation rate in general.

## ACKNOWLEDGEMENTS

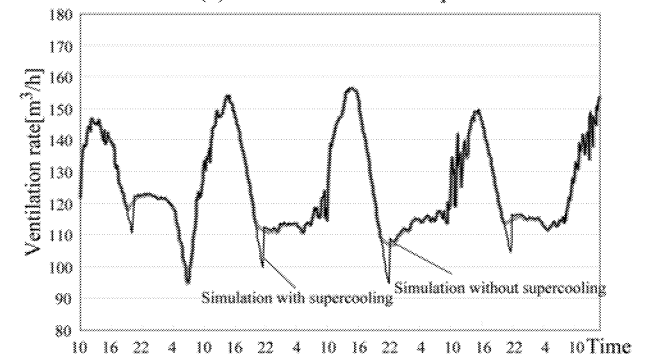
This work was partly supported by a Grant for Exploratory Research from the Ministry of Education, Culture, Sports, Science and Technology (No.17656183, Representative K. Sagara 2005). Sumika Plastech Co., Ltd. is gratefully acknowledged for providing the PCM for this study.



(1) Inside PCM (at the middle of the PCM panel)



(2) Surface of Aluminum panel



(3) Ventilation rate

Fig.15. The simulation results for the solar chimney.

## REFERENCES

- Adam Z., Yamanaka T., Kotani H. (2002). Mathematical model and experimental study of airflow in solar chimneys, *Proceedings of 8<sup>th</sup> International Conference on Air Distribution in Rooms (ROOMVENT 2002)*, pp.621-624
- Kaneko Y., Sagara K., Yamanaka T., Kotani H. (2006). Ventilation Performance of Solar Chimney with Built-in Latent Heat Storage, *Proceedings of 10<sup>th</sup> International Conference of Thermal Energy Conference (ECOSTOCK)*, CD-ROM
- Saito T. (1992). *Computer-Aided Heat Transfer*, Yokendo, (in Japanese)
- Tyagi V., Buddhi D. (2007). PCM thermal storage in buildings: A state of art, *Renewable & Sustainable Energy Reviews* 11, pp.1146-1166